Life Sciences 351 (2024) 122851

Contents lists available at ScienceDirect

Life Sciences

journal homepage: www.elsevier.com/locate/lifescie

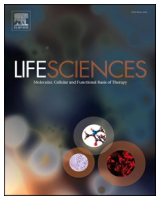

Pannexin-1 expression in tumor cells correlates with colon cancer progression and survival

Aaron Fierro-Arenas [a,c,1], Glauben Landskron [b,1], Ilan Camhi-Vainroj [a], Benjamín Basterrechea [a], Daniela Parada-Venegas [a,c], Lorena Lobos-González [d,e], Karen Dubois-Camacho [a,c], Catalina Araneda [a,b], Camila Romero [b], Antonia Domínguez [b], Gonzalo Vásquez [a,b], Francisco López-K [f], Karin Alvarez [f], Carlos M. González [g], Carolina Hager Ribeiro [h], Elisa Balboa [b], Eliseo Eugenin [i], Marcela A. Hermoso [a,c], Marjorie De la Fuente López [b,*]

[a] *Innate Immunity Laboratory, Immunology Program, Faculty of Medicine, Universidad de Chile, Santiago, Chile*
[b] *Center of Biomedical Research (CIBMED), School of Medicine, Faculty of Medicine-Clínica Las Condes, Universidad Finis Terrae, Santiago, Chile*
[c] *Department of Gastroenterology and Hepatology, University Medical Center Groningen, University of Groningen, Groningen, The Netherlands*
[d] *Regenerative Medicine Center, Faculty of Medicine, Clínica Alemana-Universidad del Desarrollo, Santiago, Chile*
[e] *Advanced Center for Chronic Diseases (ACCDiS), Faculty of Chemical and Pharmaceutical Sciences, Universidad de Chile, Santiago, Chile*
[f] *Cancer Center, Clínica Universidad de los Andes, Santiago, Chile*
[g] *School of Veterinary Medicine, Faculty of Life Sciences, Universidad Andrés Bello, Santiago, Chile*
[h] *Immunology Program, Faculty of Medicine, Universidad de Chile, Santiago, Chile*
[i] *Department of Neuroscience, Cell Biology and Anatomy, University of Texas Medical Branch (UTMB), Galveston, USA*

ARTICLE INFO

Keywords:
PANX1
Colon cancer
Cancer progression
Biomarker
Probenecid
Therapeutic targeting

ABSTRACT

Aims: Pannexin-1 (PANX1) is a hemichannel that releases ATP upon opening, initiating inflammation, cell proliferation, and migration. However, the role of PANX1 channels in colon cancer remains poorly understood, thus constituting the focus of this study.

Main methods: PANX1 mRNA expression was analyzed using multiple cancer databases. PANX1 protein expression and distribution were evaluated by immunohistochemistry on primary tumor tissue and non-tumor colonic mucosa from colon cancer patients. PANX1 inhibitors (probenecid or ^{10}Panx) were used to assess colon cancer cell lines viability. To study the role of PANX1 *in vivo*, a subcutaneous xenograft model using HCT116 cells was performed in BALB/c NOD/SCID immunodeficient mice to evaluate tumor growth under PANX1 inhibition using probenecid.

Key findings: PANX1 mRNA was upregulated in colon cancer tissue compared to non-tumor colonic mucosa. Elevated *PANX1* mRNA expression in tumors correlated with worse disease-free survival. PANX1 protein abundance was increased on tumor cells compared to epithelial cells in paired samples, in a cancer stage-dependent manner. *In vitro* and *in vivo* experiments indicated that blocking PANX1 reduced cell viability and tumor growth.

Significance: PANX1 can be used as a biomarker of colon cancer progression and blocking PANX1 channel opening could be used as a potential therapeutic strategy against this disease.

Abbreviations: Pannexin-1, (PANX1); Probenecid, (PBN); Adenosine triphosphate, (ATP); Tissue microarrays, (TMAs); Immunohistochemistry, (IHC); The Cancer Genome Atlas, (TCGA); Colon Adenocarcinoma, (COAD); Tumor-associated macrophages, (TAMs); Cancer-associated fibroblasts, (CAFs); Hours, (h)..

* Corresponding author at: Pedro de Valdivia #1509, Providencia, Santiago, Chile.
E-mail address: mdelafuente@uft.cl (M. De la Fuente López).

[1] These authors contributed equally to this work.

https://doi.org/10.1016/j.lfs.2024.122851
Received 5 February 2024; Received in revised form 11 June 2024; Accepted 14 June 2024
Available online 17 June 2024

1. Introduction

Colorectal cancer is the third most frequent cancer in the world population and the second leading cause of death by cancer, with 1.9 million new cases each year [1]. Diagnosis usually occurs in advanced stages, wherein 15–25 % of patients already manifest liver metastasis. [2]. Currently, there are few biomarkers of early and late stages of colorectal cancer [3]. High extracellular concentrations of adenosine triphosphate (ATP) have been involved with signaling pathways associated with cancer promotion, such as patient immune response, tumor cell proliferation, and metastasis [4,5]. ATP has been proposed to be a biomarker of disease in HIV-associated dementia [6]; however, whether ATP and its mechanisms of release into the extracellular milieu are associated with colorectal cancer progression is still unknown.

ATP is released into the extracellular space *via* secretory vesicles or channels, such as Pannexin-1 (PANX1) [7]. The increase in extracellular ATP levels activates purinergic receptors, which are involved in various carcinogenic cellular processes, such as proliferation, differentiation, migration, and immune response [8]. PANX1 is a heptameric hemichannel that acts as a large transmembrane pore, which upon opening, releases signaling molecules, such as ATP, into the extracellular milieu [9,10]. The channel is constitutively closed and can be activated by different stimuli, such as voltage changes, high concentrations of extracellular K^+ or intracellular Ca^{2+}, and alterations in membrane tension [11,12], possibly *via* phosphorylation by activated calcium-calmodulin-dependent protein kinase II [13], which has been shown to promote cell migration [14]. PANX1 is ubiquitously expressed in most mammalian cells, including colonic epithelium and immune cells, like macrophages and T cells [14,15]. The activity and overexpression of PANX1 have been identified in various types of cancers, such as breast cancer, hepatocellular carcinoma, leukemia, and melanoma, among others [16]. Specifically, PANX1 overexpression is related to epithelial-mesenchymal transition in gastric cancer cells [17], promotion of cell invasion and migration in hepatocellular carcinoma [18], and poor overall survival in breast cancer patients [19]. Moreover, PANX1 depletion in melanoma cell lines reduced cell migration and proliferation [20]. Nevertheless, evidence linking PANX1 to the pathogenesis of colorectal cancer is limited.

To gain deeper insights into the role of PANX1 in colon cancer progression, our study analyzed its abundance at both transcript and protein expression in human colon cancer. Additionally, we studied the effect of PANX1 blockade on a murine model of colon cancer. Our findings provide evidence that PANX1 may serve as a biomarker of cancer aggressiveness and that the utilization of PANX1 blockers could offer an alternative or adjuvant treatment to prevent cancer progression.

2. Materials and methods

2.1. Human samples

This retrospective study analyzed biological samples from patients who underwent colon cancer surgery and participated in a previous study (Fondecyt 3150328) conducted from November 2014 to October 2017 at Clínica Las Condes, Santiago, Chile [21]. Patients receiving radiation or chemotherapy prior to surgery were excluded. Tumor staging was categorized by a qualified pathologist according to the tumor–node–metastases (TNM) classification of the Union for International Cancer Control [22]. Tumor and paired non-tumor colonic mucosa from 26 patients were arranged in tissue microarrays. The selected areas corresponded to tumor cores; neither the infiltration/expansion border nor the areas of tumor surface were considered. All participants provided informed consent. The study was approved by the Medical Direction and Local Ethics Committee of Clínica Las Condes (certified AA15122014 and O22019) and Universidad Finis Terrae (No. 38-13-2021) and was performed according to human experimental guidelines. Clinical investigations were conducted according to the Declaration of Helsinki principles, with participants identified only by numbers.

2.2. Tissue microarrays (TMAs)

TMAs of human samples were assembled from paraformaldehyde-fixed, paraffin-embedded tissues using a 0.6 mm diameter punch (Beecher Instruments, Silver Spring, MD, USA). Each microarray encompassed 24 tumor cores or paired non-tumor colonic mucosa derived from colon cancer patients. Two cores from kidney tissue were used for orientation purposes. Using a tape-transfer system (Instrumedics, Hackensack, NJ, USA), 3 μm sections were transferred to glass slides and analyzed by immunohistochemistry.

2.3. Analysis of human databases of colon cancer samples

Available data from The Cancer Genome Atlas (TCGA) and GTEx databases related to *PANX1* mRNA expression levels, tissue types, patient overall survival and disease-free survival from Colon Adenocarcinoma (COAD) samples were retrieved using the XENA functional genomics explorer (http://xenabrowser.net, accessed on Dec 14th, 2023). With GEPIA2 web server (http://gepia2.cancer-pku.cn/#index, accessed on Nov 28th, 2022) [23] we queried the differential gene expression, expressed as normalized transcripts per kilobase million (nTPM) of *PANX1* from normal left colon tissue compared with normal right colon tissue from the GTEx database. Using the XENA platform, we compared *PANX1* gene expression data between tumor tissue and normal colon samples from TCGA data. Gene expression was expressed as $\log_2$(normalized_count+1). Additionally, we compared *PANX1* gene expression according to cancer stage. We analyzed patient survival data using the XENA platform based on single gene expression analysis of *PANX1* using a cutoff of >8.721 $\log_2$(norm_count+1) for the 75th percentile and < 8.169 $\log_2$(norm_count+1) for the 25th percentile, stratifying patients by the highest (Q75) and the lowest (Q25) PANX1 transcript levels.

2.4. Cancer xenograft model

Animal studies were conducted in accordance with the guidelines of the National Research and Development Agency of Chile (Agencia Nacional de Investigación y Desarrollo de Chile) and approved by the Ethical Committee of Universidad Del Desarrollo (N°10/2019). BALB/c NOD/SCID female 6–8 weeks old mice were obtained from The Jackson Laboratory (Bar Harbor, ME, USA) and maintained under specific pathogen-free conditions in a temperature-controlled room with 12/12 h light/dark schedule with food and water *ad libitum*. Mice were injected subcutaneously with 10×10^6 of the human colon cancer cell line HCT116 (American Type Culture Collection, Manassas, VA, USA) in physiological saline solution with Geltrex LDEV-Free solution (#A1413302, Gibco) on the right flank (1:1), which we considered as day 0 of the experiment. When tumors reached a volume of approximately 20 to 50 mm^3 on day 22, mice were randomized into two groups and received intraperitoneal injections with either probenecid (PBN) (300 mg per kilogram of body weight diluted in 300 μL phosphate-buffered saline (PBS) 1×) or the vehicle (300 μL PBS 1×), one injection daily until the day 25. PBN (Sigma-Aldrich, Bornem, Belgium) was solubilized in 0.5 mol/L NaOH and then diluted with PBS and buffered to pH 7.4 with HCl, as previously described [24]. Tumor growth was monitored every day for 25 days with a caliper; tumor volumes were calculated based on the following formula: tumor volume = (width x width) x length x 0.5236. Next, tumors were extracted, fixed in paraformaldehyde, weighed and then embedded in paraffin. Subsequently, 3 μm sections were stained with hematoxylin-eosin and scanned using Aperio Scanscope equipment. Finally, in the scanned slides, the percentage of the necrotic area was analyzed in relation to the total area of the tumor with Image ProPlus 4.5 morphometric software, as described

in previous studies [25,26]. Additionally, tissue sections were transferred to glass slides and analyzed by immunohistochemistry.

2.5. Immunohistochemistry (IHC)

TMA or tumor xenograft sections of 3 μm were deparaffinized and rehydrated to perform heat-induced epitope retrieval in citrate buffer (pH 6.0). Samples were further exposed to 3 % hydrogen peroxide for 10 min to block endogenous peroxidase activity. Next, the sections were incubated with 2,5 % normal horse serum for 20 min to block nonspecific reactivity, after which they were incubated overnight at 4 °C with primary antibodies to human PANX1 (1:50, ab139715, Abcam, Cambridge, MA, USA), α-SMA (1:500, A2547, Sigma–Aldrich, St. Louis, MO, USA), CD163 (ab87099; Abcam, Cambridge, MA, USA), or Ki67 (1:200, ab16667, Abcam, Cambridge, United Kingdom). Next, immunodetection of the primary antibody was conducted with the VECTASTAIN® Elite ABC-HRP Kit (PK-7200, Vector Laboratories, Burlingame, CA, USA), according to the manufacturer's instructions, and using 3,3′-diaminobenzidine as a chromogen. Finally, the sections were counterstained with hematoxylin, cleared, and mounted. The stained slides underwent scanning using Aperio ScanScope equipment, and image analysis was conducted utilizing Aperio ImageScope software, employing the Positive Pixel Count 9 algorithm. The ratio of positive pixels to the total number of pixels within a determined and equal area in all the samples (positivity per area) was considered as the abundance of the immunodetected protein, expressed in arbitrary units, which was used for comparisons and associations within this study. Negative controls were tested with each batch of patients/study slides [21]. For tumor xenografts, images were analyzed utilizing Qupath (Version 0.4.4) software, employing the "detection of positive cell" function, and the percentage of positive cells was calculated from whole tissue samples.

2.6. Immunofluorescence

HCT116 cells were seeded in a coverslip for 24 h and then fixed using 4 % paraformaldehyde in PBS (pH 7.4) for 10 min at room temperature. The cells were then incubated with 100 mM glycine and 2 % bovine serum albumin (BSA) (Sigma–Aldrich, St. Louis, MO, USA) in PBS (Sigma–Aldrich). Subsequently, the cells were incubated for 1 h at room temperature with anti-human PANX1 antibody (1:50, #710184, Invitrogen, Thermo Fisher Scientific, Waltham, MA, USA). After PBS rinse, the cells were incubated for 1 h at room temperature with a donkey anti-rabbit IgG conjugated with Alexa Fluor 488 (1:200, #A-21206 Invitrogen). Hoechst 33342 (1:500, #62249, Thermo Fisher Scientific, Rockford, IL, USA) was used as a nuclear counterstain. Finally, the slides were covered with Dako Fluorescence Mounting Medium (S302380, Agilent Technologies Inc., Santa Clara, CA, USA) and visualized with C2+ confocal microscope with 20× and 60× objectives (Nikon Instruments Inc., Melville, NY, USA).

2.7. Cell viability analysis

HCT116 and SW480 cell lines were cultured in DMEM medium (Cytiva, SH30243.02, Logan, Utah) containing 10 % heat-inactivated fetal bovine serum (FBS) (Sigma-Aldrich, F0926, United States) and antibiotic-antimycotic 1× (Gibco, 15240062), at 37 °C in a humidified atmosphere with 5 % CO_2. HCT116 cells were seeded in triplicates at a density of 10×10^3 cells per well in Falcon® 96-well Clear Flat Bottom (#353072, Corning Life Sciences) plates containing 100 μL culture medium (1 % FBS) and allowed to adhere in a 5 % CO_2 incubator at 37 °C overnight. Thereafter, cells were treated with either 0.5–2 mM PBN (#P8761, Sigma-Aldrich), 200 μM ^{10}Panx (#3348, Tocris, United Kingdom) or PBS (vehicle) as a control condition for 24, 48 and 72 h. Similarly, SW480 cells were seeded at a density of 10×10^3 cells/100 μL in 96-well plates that contained culture medium (10 % FBS), allowing them to adhere overnight. Following that, the cells were subjected to treatment with either 0.5–2 mM PBN or PBS. Cell viability was evaluated using the MTT assay kit (ab211091, Abcam, USA). Optical densities (OD) were measured at a wavelength of 590 nm using an Infinite M nano microplate reader (TECAN, Austria, GmbH).

2.8. Statistical analysis

For the comparison of *PANX1* mRNA expression between normal and tumor tissue in the TCGA database, statistical analysis of the data was performed using the non-parametric Mann-Whitney test. *PANX1* transcriptome from the TCGA database stratified by stage was analyzed with the Kruskal Wallis test. Additionally, patient survival data based on *PANX1* mRNA expression was analyzed using the Mantel-Cox test. To compare PANX1 protein abundance in paired samples (healthy mucosa and tumor tissue from colon cancer patients), the non-parametric Wilcoxon match-paired test was used. Differences between two unpaired groups (right- *vs.* left-sided colon cancer/ TNM stages I/II *vs.* III/ murine model control *vs.* PBN) were analyzed using the non-parametric Mann-Whitney test. To evaluate the correlation between PANX1 abundance and tumor T category, CD163, or α-SMA expression, the Spearman test was used. We used the Kruskal-Wallis test with Dunn's multiple comparisons to compare the viability of colon cancer cell lines treated with PBN (0.5–2 mM) or the control condition. To compare the viability of cells treated with ^{10}Panx or the vehicle, we performed the Mann-Whitney test. In every case, p values<0.05 were considered significant. GraphPad Prism 10.1.1 software was employed for data statistics.

3. Results

3.1. High PANX1 mRNA expression is related to poor prognosis in colorectal cancer

PANX1 has been associated with tumorigenic processes, including tumor cell migration and proliferation in different cancer models; however, there is limited evidence regarding its relationship with colon cancer. Therefore, we first explored available data from TCGA and GTEx databases on *PANX1* mRNA expression levels using the GEPIA2 web server (http://gepia2.cancer-pku.cn/#index, accessed November 28th, 2022) [23] and XENA functional genomics explorer (https://xenabrowser.net/, accessed December 14th, 2023) for survival analysis [27]. When analyzing colon cancer transcriptome data from TCGA, we found increased *PANX1* mRNA levels in tumor samples compared to non-tumor mucosal tissue (Fig. 1A). Afterward, we compared *PANX1* mRNA expression throughout the different stages of colon cancer, finding similar *PANX1* transcript content among groups (Fig. 1B). When stratifying colon cancer patients according to their *PANX-1* transcript levels, we observed worse disease-free survival in those patients belonging to the highest quartile compared to those in the lowest quartile ($p = 0.0412$), while overall survival was not affected (Fig. 1C and D).

In our study, we also analyzed PANX1 at the protein level in tumor biopsies and paired non-tumor colonic mucosa from 26 colon cancer patients. Demographical and clinical characteristics of the patients are described in Table 1. Thirteen of the 26 individuals were diagnosed with local metastasis to lymph nodes, and none had distant metastasis. We conducted immunohistochemical (IHC) analysis to measure PANX1 expression in tumor samples, discerning between tumor cells and stroma within the tumor area. Furthermore, we examined paired non-tumor colonic mucosa, distinguishing between epithelial cells and lamina propria (Fig. 2A). We detected higher PANX1 content in tumor cells [median (interquartile range)] [0.2100 (0.1300–0.4525)] compared to epithelial cells from non-tumor tissue [0.1900 (0.1000–0.2925)] ($p = 0.0110$) (Fig. 2B). Nonetheless, PANX1 expression was similar between the lamina propria [0.1950 (0.1600–0.3025)] and stroma [0.2300 (0.1375–0.3750)] from non-tumor and tumor regions, respectively (Fig. 2C). For visualization, the patients were color-coded according to

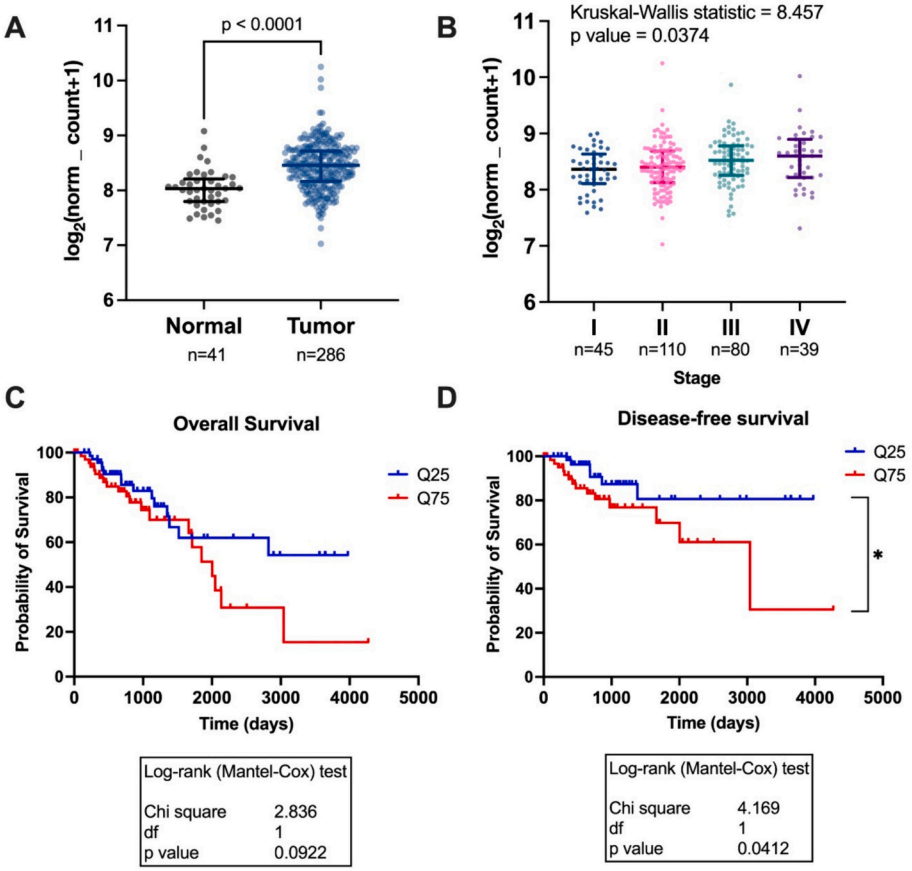

Fig. 1. *PANX1* mRNA expression in colon cancer according to TCGA transcriptome databases. (A) Abundance of *PANX1* expressed as $\log_2$(norm_count+1) in normal colon tissue or tumor and the median values with interquartile range, analyzed with Mann-Whitney test. (B) *PANX1* mRNA expression from the TCGA database stratified by stage was expressed as $\log_2$(norm_count+1) with interquartile range, analyzed with the Kruskal Wallis test. (C) Overall survival (OS) and (D) Disease-Free Survival (DFS) were depicted as Kaplan-Meier curves and estimated using a Cox proportional hazards model based on the stratification of *PANX1* expression values in colon cancer patients. The stratification was done using the gene expression data with cutoff values at the third quartile (Q75) for the high PANX1 group ($n = 67$) and the first quartile (Q25) for the low PANX1 group (n = 67). * $p < 0.05$.

Table 1
Clinical and demographic characteristics of colon cancer patients studied.

	Patients ($n = 26$)
Gender	
Female/male	8/18
Age median (range, years)	67 (33–91)
Localization	
Right/left	10/16
Tumor stage	
In situ	1
I	5
II	7
III	13
IV	0

the tumor stage, showing a bimodal distribution in tumor cells, in which those patients with TNM III stage presented higher PANX1 expression than patients in stage I or II.

3.2. The abundance of PANX1 is linked to colon cancer features associated with poor prognosis

PANX1 content in tumors has been positively correlated to the TNM staging in hepatocellular carcinoma [18]. However, an association between PANX1 protein expression and colon cancer progression has not been described yet. Therefore, we studied the relationship between the content of PANX1 in tumor cells or stroma and the pathological features of the patients. We identified a higher abundance of PANX1 in tumor cells (Fig. 3A) and stroma (Fig. 3B) from patients with TNM III, which implies lymph node compromise, compared to patients in early stages of cancer (TNM I and II) ($p = 0.0220$; $p = 0.0206$, respectively). Color-coding our study population by tumor location indicated that the patients with tumors on the right side of the colon had the highest PANX1 expression. Moreover, PANX1 protein content in tumor cells (Fig. 3C) and stroma (Fig. 3D) from tumor samples showed a positive correlation with tumor size (T category) ($r = 0.3382$, $p = 0.0491$; $r = 0.4192$, $p = 0.0185$, respectively).

A relevant characteristic in colon cancer is the location of the tumor, since tumors located on the right side (proximal colon) are associated with a more aggressive phenotype than those located on the left side [28]. For that reason, we compared PANX1 abundance in tumor cells and stroma from left or right-sided colon tumors. PANX1 abundance in both, tumor [0.4250 (0.2100–0.6200)] and stromal cells [0.3250 (0.2125–0.4825) from right-sided colon tumors was higher than that observed in left-sided colon tumors (tumor cells [0.1600 (0.0875–0.2275)] and stroma [0.1850 (0.0850 ± 0.3075)]) (Fig. 4A–B). PANX1 abundance did not show significant differences in the samples of paired non-tumor mucosa from left and right colon (Supplementary Fig. 1A-B). Additionally, when the GTEx database was analyzed, we found lower *PANX1* mRNA levels in non-affected samples from right-sided colon samples compared to left-sided samples (Supplementary Fig. 1C).

Given its ubiquitous expression, PANX1 channels may impact not

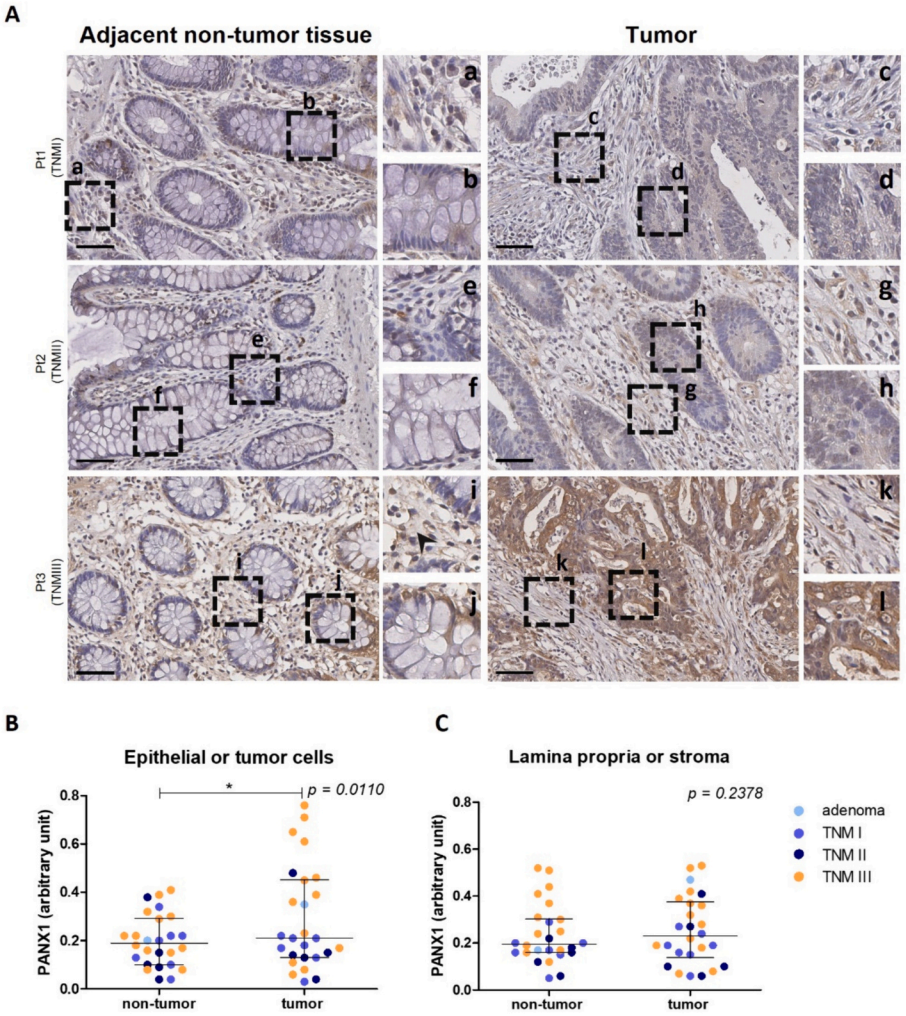

Fig. 2. PANX1 is highly expressed in human colon tumors compared to adjacent non-tumor tissue. (A) Representative image of single labeling immunohistochemistry of PANX1 in non-tumor mucosa and tumor from three colon cancer patients (Pt) with TNM I, II, or III. Magnification of 40× (bar 60 μm). Boxes a-l show zoom-in areas of epithelium/lamina propria or tumor cell/stroma in healthy or tumor tissue, respectively. (B–C) PANX1 protein expression in healthy colon and tumor samples distinguishing between epithelial/tumor cells and lamina propria/stroma, respectively. Graphs represent the abundance of PANX1 (positivity in arbitrary units) in each sample and the median values with interquartile range, analyzed with the non-parametric Wilcoxon matched pair test, * $p < 0.05$, (n = 26). For each patient, we color-coded the data based on tumor stage as a preliminary indicator of the relationship between PANX1 abundance and TNM.

only tumor cells but also neighbor cells by releasing signals with autocrine and paracrine effects. This can modulate the tumor microenvironment (TME) and potentially influence the infiltration and differentiation of cells, such as tumor-associated macrophages (TAMs) or cancer-associated fibroblasts (CAFs), which are known to present tumor-promoting states that facilitate the survival and invasiveness of cancer cells [29]. To evaluate the relationship between PANX1 in tumor tissue and the composition of the TME, we performed a correlation analysis of the stromal or tumor cell PANX1 expression with pro-tumor M2-type TAMs and CAFs markers, CD163 and α-smooth muscle actin (α-SMA), respectively. Our analysis showed that PANX1 in tumor cells correlated positively with higher α-SMA content (Spearman $r = 0.3892$, $p = 0.0494$) (Fig. 5). On the other hand, no correlation was identified between PANX1 and CD163.

3.3. PANX1 promotes tumor cell proliferation in a colon cancer cell line

To study the role of PANX1 in colon cancer progression in an *in vitro* model, we used the human colon cancer cell line HCT116, which originated from the ascending colon (right colon), is characterized by high aggressiveness and has been shown to express PANX1 [30,31]. The PANX1 subcellular localization in HCT116 cells showed a cytoplasmic and plasma membrane distribution with a speckled pattern by immunofluorescence (Fig. 6A). Since the inhibition of PANX1 has been shown to reduce the proliferation of melanoma and breast cancer cells [20,32], we evaluated the role of PANX1 in the cell viability of HCT116 colon cancer cells by using the PANX1 pharmacological inhibitor probenecid (PBN) at 0.5, 1 and 2 mM concentrations. These concentrations were selected based on previous reports demonstrating effective PANX1 inhibition without inducing cell cytotoxicity [20], as well as our own cytotoxicity assays, which confirmed the absence of cytotoxic effects in our cancer cell lines (Supplementary Table 1). PBN at 1 mM and 2 mM significantly decreased cell viability of HCT116 cells after 48 and 72 h of incubation; however, no effect was observed at 24 h (Fig. 6B–D). Cell viability curves (Fig. 6E) indicated that cell growth increased in the control condition over time, while the cells treated with PBN showed slower growth rates, depending on the concentration of the drug. Similarly, PBN at 2 mM led to a significant reduction of SW480 cell viability (Supplementary Fig. 2), which is a colon cancer cell line that was originated from an earlier-stage, less aggressive tumor and has also been shown to express PANX1 [31,33]. Additionally, ^{10}Panx, a specific PANX1 mimetic inhibitory peptide, reduced HCT116 cell viability at 48 and 72 h post incubation (Fig. 6F–I).

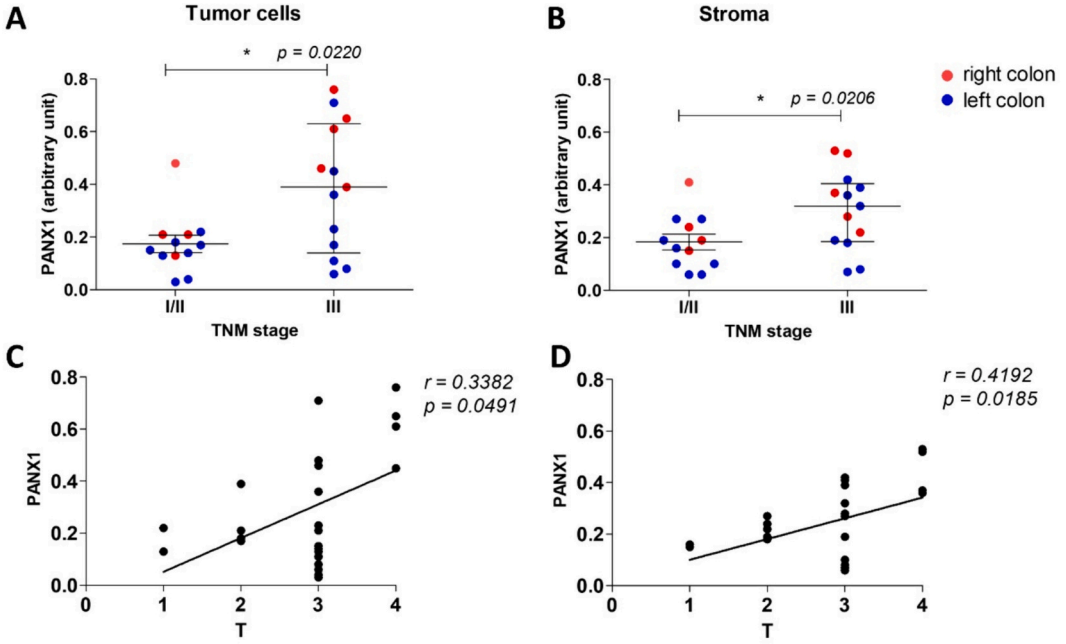

Fig. 3. PANX1 protein expression in tumor samples correlates with tumor progression. (A–B) Comparison of PANX1 expression (tumor cells and stroma, respectively) according to TNM stages I/II (n = 12) and III (n = 13). Graphs represent the PANX1 protein abundance in each sample and the median with an interquartile range, analyzed with the non-parametric Mann-Whitney test, * $p < 0.05$. For each patient, we color-coded the data according to the tumor location (right or left-sided). (C–D) The graphs show PANX1 abundance (positivity in arbitrary units) in each sample according to T category. The correlation between PANX1 expression in tumor cells (C) and stroma (D) with T category was assessed using the Spearman test, r = correlation coefficient (n = 25).

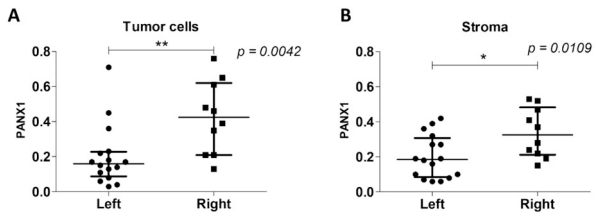

Fig. 4. The abundance of PANX1 in right-sided colon cancer tumors is higher in both (A) tumor cells and (B) stroma compared to left-sided tumors. Graphs represent the PANX1 abundance (in arbitrary units) in each sample and the median value with interquartile range, analyzed with the non-parametric Mann-Whitney test; * $p < 0.05$; ** $p < 0.01$ (left and right-sided tumors, n = 16 and 10, respectively) .

3.4. Probenecid reduces tumor growth in an HCT116 xenograft model of colon cancer

To evaluate the capacity of PANX1 inhibition to suppress tumor growth, BALB/c NOD/SCID mice were subcutaneously injected with HCT116 cells to induce ectopic tumor formation; PBN treatment or vehicle started when animals showed palpable tumors at day 22 since cell line inoculation (Fig. 7A). We observed a sustained tumor volume growth in control animals since day 23 (black triangles), while mice treated with PBN showed a decelerated tumor growth (orange circles) (Fig. 7B), which was significantly lower compared to the control group on day 25 of the experiment (Fig. 7C). Representative images of tumors from each group are shown in Fig. 7D. Tumor weight did not differ between the control and PBN groups (Fig. 7E). The analysis of the necrotic area relative to the total tumor area of hematoxylin-eosin-stained tumor samples (Supplementary Fig. 3) displayed a higher necrosis area in tumors from animals treated with PBN (Fig. 7F). We also evaluated the Ki67 expression in tumor samples through IHC as an indicator of cell proliferation (Supplementary Fig. 4). We found that

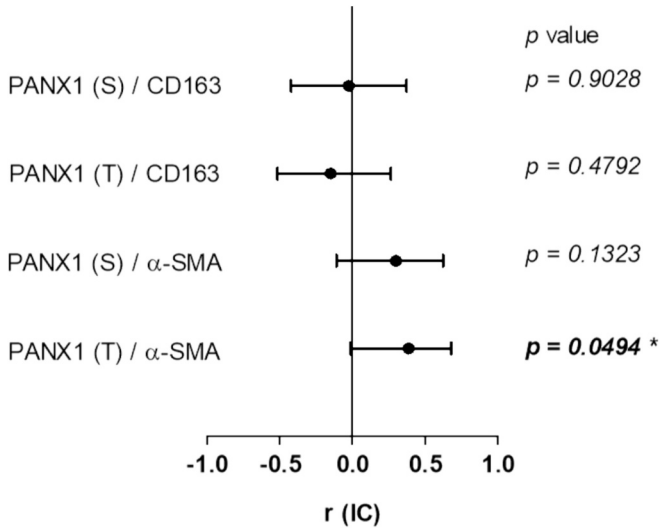

Fig. 5. PANX1 protein expression in tumor cells shows a positive correlation with α-SMA abundance in tumors. The relationship between PANX1 immunostaining in tumor (T) or stroma (S) cells and markers of CAF (α-SMA) or M2-type macrophages (CD163) was evaluated in primary tumor tissues. Spearman correlation test was performed, r coefficient and interval of confidence are depicted for each variable, * $p < 0.05$.

tumors from mice treated with PBN had a lower percentage of Ki67-positive cells compared to the control group (Fig. 7G). These results suggest that PBN treatment reduces cell proliferation and increases necrosis in the tumor.

4. Discussion

PANX1, a hemichannel that allows the release of ATP into the extracellular milieu, plays a crucial role in the progression of different

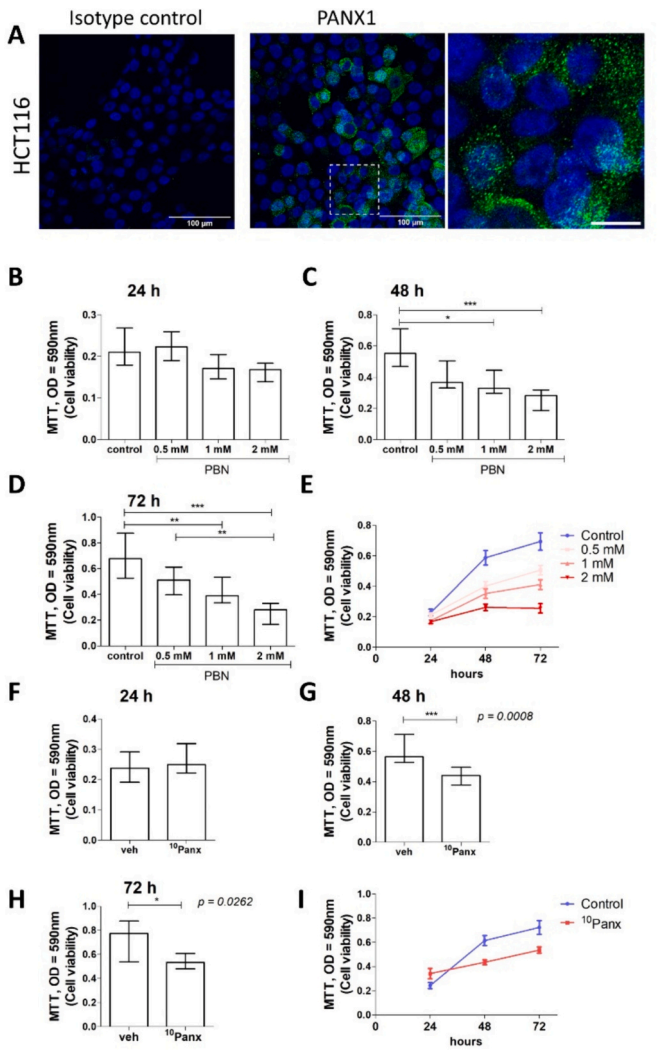

Fig. 6. The pharmacological blocking of PANX1 reduces the proliferation of HCT116 cells, assessed by the MTT assay. (A) PANX1 (green) immunofluorescence in HCT116 cells. Hoechst was used for nuclear counterstaining. The right panel displays a magnified area (scale bar of 20 μm). (B–D) Viability of HCT116 cells treated with PBN (0.5–2 mM) for 24, 48 or 72 h, respectively. Graphs represent the OD = 590 nm and the median values with interquartile range from at least three independent experiments in triplicate. Kruskal-Wallis test with Dunn's multiple comparisons were performed (* $p < 0.05$, ** $p < 0.01$, *** $p < 0.001$). (E) Cell viability curves over time for each PBN concentration and control, according to the MTT assay. (F–H) Viability of HCT116 cells treated with ^{10}Panx (200 μM) for 24, 48 and 72 h. Graphs represent the OD = 590 nm and the median values with interquartile range from at least three independent experiments in triplicate. Mann-Whitney test was performed to analyze the differences between groups (* $p < 0.05$, *** $p < 0.001$). (I) Cell viability curves over time for ^{10}Panx and control conditions, according to the MTT assay.

cancers, including melanoma and breast cancer [16]. Additionally, it has been proposed as a prognostic biomarker in pancreatic cancer [34]. However, our comprehension of PANX1 involvement in colon cancer remains limited, with sparse research available thus far, being suggested to induce pyroptosis in colon cancer cells [30] and modulate the anti-tumor immune response after chemotherapy [33]. Therefore, our study aimed to assess the potential role of PANX1 in the progression of human colon cancer.

Previous studies using different databases have shown that mRNA levels of *PANX1* are increased in various types of tumors, including colorectal cancer [34,35]. Our *in-silico* analysis showed that PANX1 not only has a higher mRNA expression in colon cancer compared to non-tumor tissue, but its overexpression is associated with worse overall survival, which could be pointing to a role for PANX1 in the severity of this disease. Similarly, high expression of PANX1 has been associated with poor prognosis in patients with lung and pancreatic adenocarcinoma, kidney renal papillary cell carcinoma, and breast cancers [19,34], suggesting that it has potential value as a prognostic biomarker.

In the present report, we studied the protein abundance of PANX1 in biopsies from colon cancer patients through IHC, distinguishing between tumor and stromal compartments. Due to its ubiquitous expression and its role in cellular communication, the pattern of PANX1 expression in the different tumor tissue compartments, as described here, could be key to understanding its role in colon cancer progression. Previously, immunohistochemical localization analysis of PANX1 in healthy human colon demonstrated that PANX1 immunoreactivity was present in all layers of the colon tissue, where it showed a cytoplasmic and membrane pattern in the epithelial and goblet cells, while it was also present in a variety of cells of the lamina propria, such as polymorphonuclear leukocytes, nerve fibers, and small blood vessels [36]. Our analysis carried out on biopsies from patients with colon cancer allowed us to identify higher PANX1 protein expression in tumor cells compared to the healthy epithelium. Furthermore, the expression of PANX1 in both tumor and stromal cells is directly associated with the stages of the disease, with higher expression of PANX1 in patients with lymph node compromise. These findings are in line with previous studies in other types of cancer, as PANX1 is overexpressed in human melanoma [20] and its expression is directly associated with a worse prognosis for hepatocellular carcinoma patients [18]. Moreover, PANX1 upregulation was found to have a positive correlation with the expression of genes related to the epithelial-to-mesenchymal transition pathway in breast and gastric cancer cell lines, contributing to an increased metastatic potential of cancer cells [17,32]. Unfortunately, we were unable to assess the correlation between PANX1 and colon cancer metastasis to distant organs, because our study cohort did not include cases involving such pathological feature, and our murine xenograft model did not exhibit cancerous invasion of distant organs. However, this aspect warrants further exploration in future studies.

We hypothesize that the increase of PANX1 might result in increased ATP concentrations in the TME of colon cancer, as seen in breast cancer [35], which could potentially stimulate the proliferation and migration of colon cancer cells to other tissues, such as lymph nodes. Previous reports have demonstrated that the ATP release with subsequent autocrine activation of P2 purinergic receptors, such as P2X7R, promotes the motility and migration of human lung cancer cells *in vitro* [37], in a similar way to what has been shown in dendritic cells, for which autocrine ATP-stimulation induces fast migration in a PANX1-P2X7R-Ca^{2+} signaling dependent manner [38].

Our findings suggesting PANX1 involvement in tumor progression are further supported by our experiments employing the PANX1 blocking agent PBN in colon cancer-derived cell lines (HCT116 and SW480), which appears to decrease cell proliferation *in vitro*. Likewise, evidence shows that pharmacological blockade or genetic suppression of PANX1 reduces cell proliferation, migration, and epithelial-to-mesenchymal transition, while its overexpression increases invasiveness in different cancer models [17,20,32,39]. The impact of PANX1 inhibition on cell viability in our study varied depending on the specific cell line under investigation, with the highly aggressive HCT116 cells being more sensitive to lower concentrations of PBN than the SW480 cells, suggesting that the reduction in the proliferation of tumor cells when inhibiting PANX1 with PBN depends on the tumor's pathological characteristics, such as its stage. Based on our results, the use of PANX1 blockers may become an attractive therapeutical strategy that should be further investigated to support the management and treatment of colon cancer patients. However, given the heterogeneity of patients, it will be essential to delve into tumor characteristics that hint at which patients would be responsive to PANX1 blockade.

PBN is a drug that inhibits PANX1 channel function by interacting

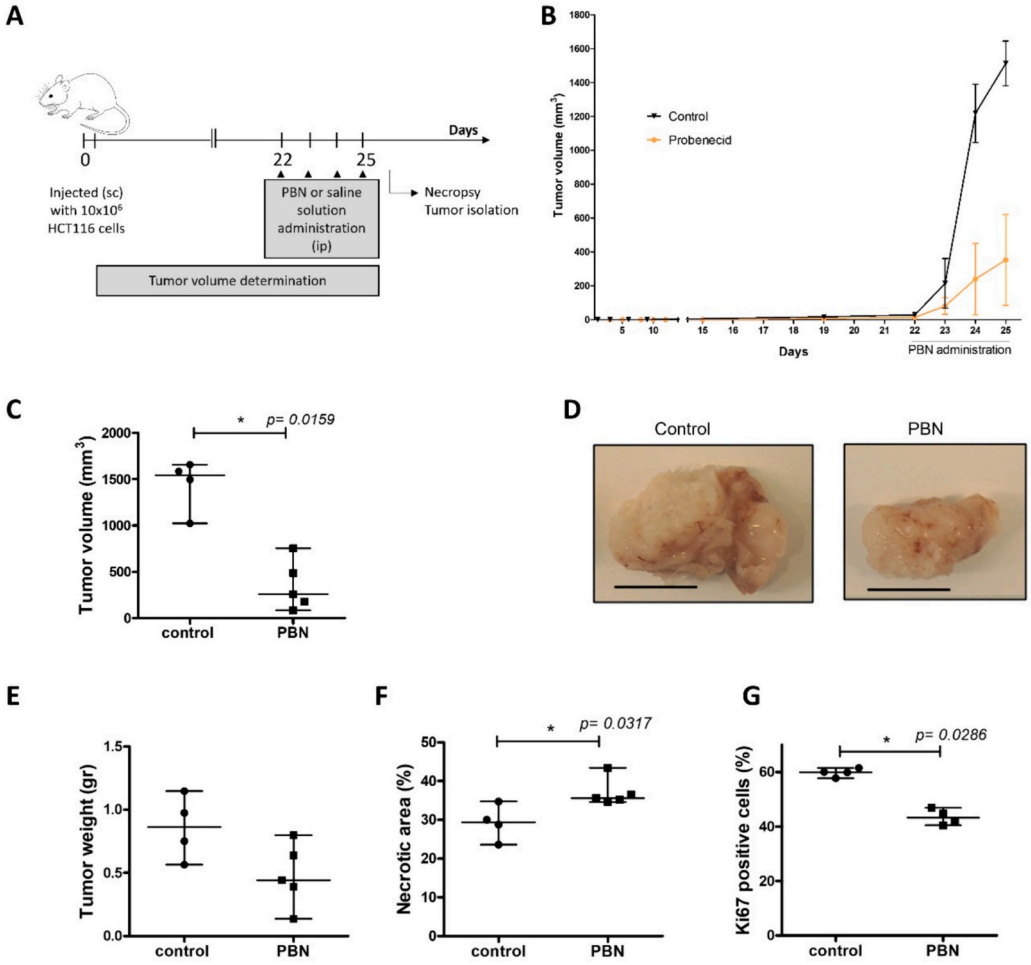

Fig. 7. PBN inhibits tumor growth in a colon cancer xenograft murine model. (A) Diagram showing the time course of protocols used for tumor induction and evaluation of the effect of PANX1 pharmacological inhibitor probenecid on BALB/c NOD/SCID mice injected subcutaneously (sc) with 10×10^6 HCT116 cells in Geltrex solution (1:1) on the right flank. Mice were randomized into two groups, which received intraperitoneal (ip) injections with PBN or PBS once a day. Tumor volume was monitored every day. (B) Tumor volume curves over time in animals treated with PBN (orange line) or saline solution as control (black line). (C) The graph displays the tumor volume (mm^3) for both the control group and animals treated with PBN on the 25th day of the experiment. Mann-Whitney test was applied. (D) Representative images of tumors from control and PBN-treated animals. The scale bar represents 1 cm. (E) Tumor weight after tumor extraction in animals treated with PBN or control is depicted in the figure. Mann-Whitney test was applied, and no significant differences were found. (F) Necrotic area and (G) Ki67 positive cells percentage in the tumor samples from mice treated with PBN or control (Mann-Whitney test was applied, * $p < 0.05$).

with its first extracellular loop [40], it is currently approved by the FDA and utilized for the treatment of gout [41]. Previous reports indicated that the use of PBN in combination with chemotherapeutic agents enhances their antineoplastic effects, working as a chemosensitizer in cell lines of neuroblastoma, breast cancer, and cervical carcinoma [42], as well as in 3D-cultured prostate cancer cells [43]. In our xenograft model, mice treated with PBN developed tumors with reduced volume and expression of the proliferation marker Ki67, and induced higher levels of necrosis, suggesting that PANX1 may participate in the growth and viability of colon tumors, with the blockade of PANX1 potentially delaying colon cancer progression.

The modulation of the TME through ATP release by PANX1 may impact stromal cells [44,45], potentially affecting tumor progression as well. ATP in the TME has diverse effects on tumor growth, immune responses, and angiogenesis, presenting pro-tumorigenic and antitumor roles, depending on the ATP concentration, the specific receptor activation, and the cellular context [45]. Prior studies based on multiple algorithms (TIMER 2.0) evaluated the relationship between *PANX1* gene expression and TME cellular composition, demonstrating that PANX1 positively correlated with markers of CAFs, macrophages, and neutrophils in several cancer types, including colon adenocarcinoma [34]. Because of their close interaction with tumor cells, CAFs are an important actor within the TME, constituting a poor prognostic factor in multiple cancers. CAFs remodel the extracellular matrix, facilitating tumor invasion and metastases, and are key for the growth of fibrotic tissue in the tumor, caused mainly by the activation of fibroblasts into myofibroblasts, which express α-SMA as their cytoplasmic microfilaments [46]. In models of ischemia, the release of ATP through PANX1 channels in cardiomyocytes triggers a paracrine signal that activates the transformation of fibroblasts into myofibroblasts, resulting in an increase in α-SMA expression, ultimately promoting fibrosis [47]. Therefore, we studied the relationship between PANX1 and α-SMA in the TME of colon cancer, finding a positive correlation between the expression of PANX1 in tumor cells and α-SMA in the stroma. Increased PANX1 expression in colon cancer cells might result in elevated extracellular ATP levels, potentially triggering responses in other cell populations. For example, it could induce the proliferation of CAFs within the TME, thus promoting cancer invasiveness. Nevertheless, further studies are necessary to evaluate whether the inhibition of PANX1 decreases the presence of CAFs in the tumor milieu. In a similar way, we analyzed the relationship between PANX1 and $CD163^+$ M2-type TAMs, as these immune cells have been shown to be involved in invasion, migration, and metastasis of tumor cells [48] and are considered a poor prognostic factor [49]. While we did not observe a correlation between PANX1 and

CD163 expression, further experiments are required to ascertain whether PANX1 is involved in the infiltration of M2-type TAM in the tumor. Exploring this avenue is attractive, considering that the M2 macrophage phenotype has been shown to exhibit increased expression of P2X7R [50], a receptor whose activation can be induced by PANX1-released ATP [51], promoting cell migration and other responses.

Tumor location in colon cancer has been related to differential pathways of carcinogenesis, since tumors located on the right side (proximal colon) show microsatellite instability, CpG-islands-methylation phenotype, more frequent silencing of the mismatch repair gene MLH1, and are associated with aggressive phenotypes and worse prognosis than those on the left side, which are characterized by chromosomal instability [28,52]. Here, we found that tumors located on the right colon have a higher abundance of PANX1 than those on the left colon, suggesting a relationship between this hemichannel expression and the molecular pathways that are involved in right colon cancer.

5. Conclusions

Our results align and reinforce previous reports that propose a protumoral role for PANX1, as higher expression of this molecule is associated with colon cancer cell proliferation and lymph node invasion. The interaction between tumor and stromal cells may play a role in PANX1 function, resulting in the progression of colon cancer and a worse prognosis for the patient. These findings make PANX1 a promising colon cancer biomarker, although more research is needed to validate this proposal. Furthermore, a potential therapeutic strategy for colon cancer may involve the pharmacological suppression of PANX1.

Supplementary data to this article can be found online at https://doi.org/10.1016/j.lfs.2024.122851.

Ethics approval and consent to participate

The study with human samples was conducted in accordance with the Declaration of Helsinki and approved by the Institutional Ethics Committee of Clínica Las Condes (certified AA15122014 and O22019) and Universidad Finis Terrae (No. 38-13-2021). Informed consent was obtained from all subjects involved in the study. The animal study protocol was approved by the Institutional Ethics Committee of Universidad Del Desarrollo (N°10/2019).

Funding

This research was funded by The National Research and Development Agency from Chile (Agencia Nacional de Investigación y Desarrollo), Fondecyt de Iniciación #11190990 (MDF), Fondecyt Postdoc #3190931 (GL), 3210367 (KD), Fondecyt de Iniciación #11230904 (GL), #11230689 (EB), Fondecyt Regular #1220702 (MAH), Fondap ACCDiS #15130011 (LLG), Fondecyt #1211223 (LLG), and Internal funding from Universidad Finis Terrae VRICAD-FF2023 (MDF).

CRediT authorship contribution statement

Aaron Fierro-Arenas: Writing – review & editing, Writing – original draft, Visualization, Validation, Investigation, Formal analysis, Data curation. **Glauben Landskron:** Writing – review & editing, Writing – original draft, Visualization, Validation, Supervision, Resources, Methodology, Investigation, Funding acquisition, Data curation, Conceptualization. **Ilan Camhi-Vainroj:** Writing – original draft, Investigation, Formal analysis, Data curation. **Benjamín Basterrechea:** Writing – original draft, Investigation, Formal analysis, Data curation. **Daniela Parada-Venegas:** Methodology, Investigation, Data curation. **Lorena Lobos-González:** Writing – review & editing, Visualization, Validation, Resources, Methodology, Investigation, Funding acquisition, Formal analysis, Data curation, Conceptualization. **Karen Dubois-Camacho:** Writing – review & editing, Project administration, Investigation, Funding acquisition, Formal analysis, Conceptualization. **Catalina Araneda:** Methodology, Investigation, Formal analysis, Data curation. **Camila Romero:** Investigation, Formal analysis, Data curation. **Antonia Domínguez:** Methodology, Investigation, Data curation. **Francisco López-K:** Resources, Conceptualization. **Karin Alvarez:** Resources, Conceptualization. **Carlos M. González:** Methodology, Investigation, Formal analysis. **Carolina Hager Ribeiro:** Validation, Supervision, Methodology. **Elisa Balboa:** Writing – review & editing, Resources, Methodology, Investigation, Funding acquisition, Formal analysis. **Eliseo Eugenin:** Writing – review & editing, Methodology, Formal analysis, Conceptualization. **Marcela A. Hermoso:** Writing – review & editing, Validation, Supervision, Resources, Methodology, Investigation, Funding acquisition, Formal analysis, Conceptualization. **Marjorie De la Fuente López:** Writing – review & editing, Writing – original draft, Visualization, Validation, Supervision, Resources, Project administration, Methodology, Investigation, Funding acquisition, Formal analysis, Data curation, Conceptualization.

Declaration of competing interest

The authors declare that they have no known competing financial interests or personal relationships that could have appeared to influence the work reported in this paper.

Acknowledgments

The results shown here are in part based upon data generated by the TCGA Research Network: https://www.cancer.gov/tcga, through the GEPIA web server, accessed Nov 28th, 2022. The Genotype-Tissue Expression (GTEx) Project was supported by the Common Fund of the Office of the Director of the National Institutes of Health, and by NCI, NHGRI, NHLBI, NIDA, NIMH, and NINDS. The data used for the analyses described in this manuscript were obtained from the GEPIA web server that has access to the GTEx database, accessed Nov 28th, 2022.

References

[1] H. Sung, J. Ferlay, R.L. Siegel, M. Laversanne, I. Soerjomataram, A. Jemal, F. Bray, Global Cancer Statistics, GLOBOCAN estimates of incidence and mortality worldwide for 36 cancers in 185 countries, CA Cancer J. Clin. 71 (2021) (2020) 209–249, https://doi.org/10.3322/caac.21660.
[2] E.P. Ward, C.N. Clarke, Epidemiology and risk factors for metastatic colorectal disease, in: Contemp. Manag. Metastatic Color. Cancer, Elsevier, 2022, pp. 1–17, https://doi.org/10.1016/B978-0-323-91706-3.00014-X.
[3] O.O. Ogunwobi, F. Mahmood, A. Akingboye, Biomarkers in colorectal Cancer: current research and future prospects, Int. J. Mol. Sci. 21 (2020) 5311, https://doi.org/10.3390/ijms21155311.
[4] F. Di Virgilio, E. Adinolfi, Extracellular purines, purinergic receptors and tumor growth, Oncogene 36 (2017) 293–303, https://doi.org/10.1038/onc.2016.206.
[5] A.M. Chiarella, Y.K. Ryu, G.A. Manji, A.K. Rustgi, Extracellular ATP and adenosine in Cancer pathogenesis and treatment, Trends Cancer 7 (2021) 731–750, https://doi.org/10.1016/j.trecan.2021.04.008.
[6] S. Velasquez, L. Prevedel, S. Valdebenito, A.M. Gorska, M. Golovko, N. Khan, J. Geiger, E.A. Eugenin, Circulating levels of ATP is a biomarker of HIV cognitive impairment, EBioMedicine 51 (2020) 102503, https://doi.org/10.1016/j.ebiom.2019.10.029.
[7] G. Burnstock, J.-M. Boeynaems, Purinergic signalling and immune cells, Purinergic Signal 10 (2014) 529–564, https://doi.org/10.1007/s11302-014-9427-2.
[8] V. Vultaggio-Poma, A.C. Sarti, F. Di Virgilio, Extracellular ATP: a feasible target for Cancer therapy, Cells 9 (2020) 2496, https://doi.org/10.3390/cells9112496.
[9] Z. Ruan, I.J. Orozco, J. Du, W. Lü, Structures of human pannexin 1 reveal ion pathways and mechanism of gating, Nature 584 (2020) 646–651, https://doi.org/10.1038/s41586-020-2357-y.
[10] S. Velasquez, E.A. Eugenin, Role of Pannexin-1 hemichannels and purinergic receptors in the pathogenesis of human diseases, Front. Physiol. 5 MAR (2014) 1–12, https://doi.org/10.3389/fphys.2014.00096.
[11] X. López, R. Escamilla, P. Fernández, Y. Duarte, F. González-Nilo, N. Palacios-Prado, A.D. Martinez, J.C. Sáez, Stretch-induced activation of Pannexin 1 channels can be prevented by PKA-dependent phosphorylation, Int. J. Mol. Sci. 21 (2020) 9180, https://doi.org/10.3390/ijms21239180.
[12] P.W. Furlow, S. Zhang, T.D. Soong, N. Halberg, H. Goodarzi, C. Mangrum, Y.G. Wu, O. Elemento, S.F. Tavazoie, Mechanosensitive pannexin-1 channels mediate microvascular metastatic cell survival, Nat. Cell Biol. 17 (2015) 943–952, https://doi.org/10.1038/ncb3194.

[13] X. López, N. Palacios-Prado, J. Güiza, R. Escamilla, P. Fernández, J.L. Vega, M. Rojas, V. Marquez-Miranda, E. Chamorro, A.M. Cárdenas, M.C. Maldifassi, A. D. Martínez, Y. Duarte, F.D. González-Nilo, J.C. Sáez, A physiologic rise in cytoplasmic calcium ion signal increases pannexin1 channel activity via a C-terminus phosphorylation by CaMKII, Proc. Natl. Acad. Sci. 118 (2021), https://doi.org/10.1073/pnas.2108967118.
[14] P.A. Harcha, T. López-López, A.G. Palacios, P.J. Sáez, Pannexin Channel regulation of cell migration: focus on immune cells, Front. Immunol. 12 (2021), https://doi.org/10.3389/fimmu.2021.750480.
[15] S. Crespo Yanguas, J. Willebrords, S.R. Johnstone, M. Maes, E. Decrock, M. De Bock, L. Leybaert, B. Cogliati, M. Vinken, Pannexin1 as mediator of inflammation and cell death, Biochim. Biophys. Acta - Mol. Cell Res. 1864 (2017) 51–61, https://doi.org/10.1016/j.bbamcr.2016.10.006.
[16] J.X. Jiang, S. Penuela, Connexin and pannexin channels in cancer, BMC Cell Biol. 17 (2016) S12, https://doi.org/10.1186/s12860-016-0094-8.
[17] W. Ying, K. Zheng, Y. Wu, O. Wang, Pannexin 1 Mediates Gastric Cancer Cell Epithelial–Mesenchymal Transition via Aquaporin 5, Biol. Pharm. Bull. 44 (2021) b21–00292. doi:https://doi.org/10.1248/bpb.b21-00292.
[18] G. Shi, C. Liu, Y. Yang, L. Song, X. Liu, C. Wang, Z. Peng, H. Li, L. Zhong, Panx1 promotes invasion-metastasis cascade in hepatocellular carcinoma, J. Cancer 10 (2019) 5681–5688, https://doi.org/10.7150/jca.32986.
[19] M.K.G. Stewart, I. Plante, S. Penuela, D.W. Laird, Loss of Panx1 impairs mammary gland development at lactation: implications for breast tumorigenesis, PloS One 11 (2016) e0154162, https://doi.org/10.1371/journal.pone.0154162.
[20] T. Freeman, S. Sayedyahossein, D. Johnston, R. Sanchez-Pupo, B. O'Donnell, K. Huang, Z. Lakhani, D. Nouri-Nejad, K. Barr, L. Harland, S. Latosinsky, A. Grant, L. Dagnino, S. Penuela, Inhibition of Pannexin 1 reduces the tumorigenic properties of human melanoma cells, Cancers (Basel) 11 (2019) 102, https://doi.org/10.3390/cancers11010102.
[21] M. De la Fuente López, G. Landskron, D. Parada, K. Dubois-Camacho, D. Simian, M. Martinez, D. Romero, J.C. Roa, I. Chahuán, R. Gutiérrez, F. Lopez-K, K. Alvarez, U. Kronberg, S. López, A. Sanguinetti, N. Moreno, M. Abedrapo, M.J. González, R. Quera, M.A. Hermoso-R, The relationship between chemokines CCL2, CCL3, and CCL4 with the tumor microenvironment and tumor-associated macrophage markers in colorectal cancer, Tumour Biol. 40 (2018) 1–12, https://doi.org/10.1177/1010428318810059.
[22] L.H. Sobin, C. Wittekind, TNM Classification of Malignant Tumours, 6th edition, Wiley-Liss Publisher, New York, 2002.
[23] Z. Tang, B. Kang, C. Li, T. Chen, Z. Zhang, GEPIA2: an enhanced web server for large-scale expression profiling and interactive analysis, Nucleic Acids Res. 47 (2019) W556–W560, https://doi.org/10.1093/nar/gkz430.
[24] J.M. Miller, U. MacGarvey, M. Flint Beal, The effect of peripheral loading with kynurenine and probenecid on extracellular striatal kynurenic acid concentrations, Neurosci. Lett. 146 (1992) 115–118, https://doi.org/10.1016/0304-3940(92)90186-B.
[25] A.C. Johansson, E. Visse, B. Widegren, H.-O. Sjögren, P. Siesjö, Computerized image analysis as a tool to quantify infiltrating leukocytes, J. Histochem. Cytochem. 49 (2001) 1073–1079, https://doi.org/10.1177/002215540104900902.
[26] J.S. Francisco, H.P. de Moraes, E.P. Dias, Evaluation of the image-pro plus 4.5 software for automatic counting of labeled nuclei by PCNA immunohistochemistry, Braz. Oral Res. 18 (2004) 100–104, https://doi.org/10.1590/S1806-83242004000200002.
[27] M.J. Goldman, B. Craft, M. Hastie, K. Repečka, F. McDade, A. Kamath, A. Banerjee, Y. Luo, D. Rogers, A.N. Brooks, J. Zhu, D. Haussler, Visualizing and interpreting cancer genomics data via the Xena platform, Nat. Biotechnol. 38 (2020) 675–678, https://doi.org/10.1038/s41587-020-0546-8.
[28] M.S. Lee, D.G. Menter, S. Kopetz, Right versus left Colon Cancer biology: integrating the consensus molecular subtypes, J. Natl. Compr. Canc. Netw. 15 (2017) 411–419, https://doi.org/10.6004/jnccn.2017.0038.
[29] G. Gunaydin, CAFs interacting with TAMs in tumor microenvironment to enhance tumorigenesis and immune evasion, Front. Oncol. 11 (2021), https://doi.org/10.3389/fonc.2021.668349.
[30] V. Derangère, A. Chevriaux, F. Courtaut, M. Bruchard, H. Berger, F. Chalmin, S. Z. Causse, E. Limagne, F. Végran, S. Ladoire, B. Simon, W. Boireau, A. Hichami, L. Apetoh, G. Mignot, F. Ghiringhelli, C. Rébé, Liver X receptor β activation induces pyroptosis of human and murine colon cancer cells, Cell Death Differ. 21 (2014) 1914–1924, https://doi.org/10.1038/cdd.2014.117.
[31] D. Ahmed, P.W. Eide, I.A. Eilertsen, S.A. Danielsen, M. Eknæs, M. Hektoen, G. E. Lind, R.A. Lothe, Epigenetic and genetic features of 24 colon cancer cell lines, Oncogenesis 2 (2013) e71, https://doi.org/10.1038/oncsis.2013.35.
[32] N. Jalaleddine, L. El-Hajjar, H. Dakik, A. Shaito, J. Saliba, R. Safi, K. Zibara, M. El-Sabban, Pannexin1 is associated with enhanced epithelial-to-mesenchymal transition in human patient breast Cancer tissues and in breast Cancer cell lines, Cancers (Basel) 11 (2019) 1967, https://doi.org/10.3390/cancers11121967.
[33] K.C.-Y. Huang, S.-F. Chiang, P.-C. Lin, W.-Z. Hong, P.-C. Yang, H.-P. Chang, S.-L. Peng, T.-W. Chen, T.-W. Ke, J.-A. Liang, W.T.-L. Chen, K.S.C. Chao, TNFα modulates PANX1 activation to promote ATP release and enhance P2RX7-mediated antitumor immune responses after chemotherapy in colorectal cancer, Cell Death Dis. 15 (2024) 24, https://doi.org/10.1038/s41419-023-06408-5.
[34] L. Bao, K. Sun, X. Zhang, PANX1 is a potential prognostic biomarker associated with immune infiltration in pancreatic adenocarcinoma: a pan-cancer analysis, Channels (Austin) 15 (2021) 680–696, https://doi.org/10.1080/19336950.2021.2004758.
[35] W. Chen, B. Li, F. Jia, J. Li, H. Huang, C. Ni, W. Xia, High PANX1 expression leads to neutrophil recruitment and the formation of a high adenosine immunosuppressive tumor microenvironment in basal-like breast Cancer, Cancers (Basel) 14 (2022) 3369, https://doi.org/10.3390/cancers14143369.
[36] E.F. Diezmos, S.L. Sandow, I. Markus, D. Shevy Perera, D.Z. Lubowski, D.W. King, P.P. Bertrand, L. Liu, Expression and localization of pannexin-1 hemichannels in human colon in health and disease, Neurogastroenterol. Motil. 25 (2013) e395–e405, https://doi.org/10.1111/nmo.12130.
[37] E. Takai, M. Tsukimoto, H. Harada, S. Kojima, Autocrine signaling via release of ATP and activation of P2X7 receptor influences motile activity of human lung cancer cells, Purinergic Signal 10 (2014) 487–497, https://doi.org/10.1007/s11302-014-9411-x.
[38] P.J. Sáez, P. Vargas, K.F. Shoji, P.A. Harcha, A.-M. Lennon-Duménil, J.C. Sáez, ATP promotes the fast migration of dendritic cells through the activity of pannexin 1 channels and P2X 7 receptors, Sci. Signal. 10 (2017), https://doi.org/10.1126/scisignal.aah7107.
[39] H. Liu, M. Yuan, Y. Yao, D. Wu, S. Dong, X. Tong, In vitro effect of Pannexin 1 channel on the invasion and migration of I-10 testicular cancer cells via ERK1/2 signaling pathway, Biomed. Pharmacother. 117 (2019) 109090, https://doi.org/10.1016/j.biopha.2019.109090.
[40] K. Michalski, T. Kawate, Carbenoxolone inhibits Pannexin1 channels through interactions in the first extracellular loop, J. Gen. Physiol. 147 (2016) 165–174, https://doi.org/10.1085/jgp.201511505.
[41] W. Silverman, S. Locovei, G. Dahl, Probenecid, a gout remedy, inhibits pannexin 1 channels, Am. J. Physiol. Physiol. 295 (2008) C761–C767, https://doi.org/10.1152/ajpcell.00227.2008.
[42] D. Campos-Arroyo, J.C. Martínez-Lazcano, J. Melendez-Zajgla, Probenecid is a chemosensitizer in cancer cell lines, Cancer Chemother. Pharmacol. 69 (2012) 495–504, https://doi.org/10.1007/s00280-011-1725-6.
[43] J. Uwada, S. Mukai, N. Terada, H. Nakazawa, M.S. Islam, T. Nagai, M. Fujii, K. Yamasaki, T. Taniguchi, T. Kamoto, T. Yazawa, Pleiotropic effects of probenecid on three-dimensional cultures of prostate cancer cells, Life Sci. 278 (2021) 119554, https://doi.org/10.1016/j.lfs.2021.119554.
[44] C.L. Alvarez, M.F. Troncoso, M.V. Espelt, Extracellular ATP and adenosine in tumor microenvironment: roles in epithelial–mesenchymal transition, cell migration, and invasion, J. Cell. Physiol. 237 (2022) 389–400, https://doi.org/10.1002/jcp.30580.
[45] F. Di Virgilio, A.C. Sarti, S. Falzoni, E. De Marchi, E. Adinolfi, Extracellular ATP and P2 purinergic signalling in the tumour microenvironment, Nat. Rev. Cancer 18 (2018) 601–618, https://doi.org/10.1038/s41568-018-0037-0.
[46] D. Ganguly, R. Chandra, J. Karalis, M. Teke, T. Aguilera, R. Maddipati, M. B. Wachsmann, D. Ghersi, G. Siravegna, H.J. Zeh, R. Brekken, D.T. Ting, M. Ligorio, Cancer-associated fibroblasts: versatile players in the tumor microenvironment, Cancers (Basel) 12 (2020) 2652, https://doi.org/10.3390/cancers12092652.
[47] E. Dolmatova, G. Spagnol, D. Boassa, J.R. Baum, K. Keith, C. Ambrosi, M. I. Kontaridis, P.L. Sorgen, G.E. Sosinsky, H.S. Duffy, Cardiomyocyte ATP release through pannexin 1 aids in early fibroblast activation, Am. J. Physiol. Circ. Physiol. 303 (2012) H1208–H1218, https://doi.org/10.1152/ajpheart.00251.2012.
[48] Y. Komohara, Y. Fujiwara, K. Ohnishi, M. Takeya, Tumor-associated macrophages: potential therapeutic targets for anti-cancer therapy, Adv. Drug Deliv. Rev. 99 (2016) 180–185, https://doi.org/10.1016/j.addr.2015.11.009.
[49] T. Xue, K. Yan, Y. Cai, J. Sun, Z. Chen, X. Chen, W. Wu, Prognostic significance of CD163+ tumor-associated macrophages in colorectal cancer, World J. Surg. Oncol. 19 (2021) 186, https://doi.org/10.1186/s12957-021-02299-y.
[50] G. Lopez-Castejón, A. Baroja-Mazo, P. Pelegrín, Novel macrophage polarization model: from gene expression to identification of new anti-inflammatory molecules, Cell. Mol. Life Sci. 68 (2011) 3095–3107, https://doi.org/10.1007/s00018-010-0609-y.
[51] P. Pelegrin, A. Surprenant, Pannexin-1 mediates large pore formation and interleukin-1β release by the ATP-gated P2X7 receptor, EMBO J. 25 (2006) 5071–5082, https://doi.org/10.1038/sj.emboj.7601378.
[52] T. Sugai, W. Habano, Y.-F. Jiao, M. Tsukahara, Y. Takeda, K. Otsuka, S. Nakamura, Analysis of molecular alterations in left- and right-sided colorectal carcinomas reveals distinct pathways of carcinogenesis, J. Mol. Diagnostics 8 (2006) 193–201, https://doi.org/10.2353/jmoldx.2006.050052.